Separation Science and Technology
Publication details, including instructions for authors and subscription information:
http://www.informaworld.com/smpp/title~content=t713708471

Development of Spiral-Type Supported Liquid Membrane Module for Separation and Concentration of Metal Ions

Masaaki Teramoto[a]; Hideto Matsuyama[a]; Hitoshi Takaya[a]; Shigehiro Asano[a]
[a] DEPARTMENT OF INDUSTRIAL CHEMISTRY, KYOTO INSTITUTE OF TECHNOLOGY, KYOTO, JAPAN

To cite this Article Teramoto, Masaaki , Matsuyama, Hideto , Takaya, Hitoshi and Asano, Shigehiro(1987) 'Development of Spiral-Type Supported Liquid Membrane Module for Separation and Concentration of Metal Ions', Separation Science and Technology, 22: 11, 2175 — 2201
To link to this Article: DOI: 10.1080/01496398708068607
URL: http://dx.doi.org/10.1080/01496398708068607

SEPARATION SCIENCE AND TECHNOLOGY, 22(11), pp. 2175-2201, 1987

Development of Spiral-Type Supported Liquid Membrane Module for Separation and Concentration of Metal Ions

MASAAKI TERAMOTO,* HIDETO MATSUYAMA, HITOSHI TAKAYA, and SHIGEHIRO ASANO

DEPARTMENT OF INDUSTRIAL CHEMISTRY
KYOTO INSTITUTE OF TECHNOLOGY
MATSUGASAKI, SAKYO-KU, KYOTO 606, JAPAN

Abstract

Experiments on the single permeation of cobalt, nickel, and zinc, and the simultaneous permeation of cobalt and nickel were performed using newly developed spiral-type supported liquid membrane modules. These metal ions were successfully separated and concentrated. EHPNA (2-ethylhexylphosphonic acid mono-2-ethylhexyl ester) was used as the carrier of cobalt and nickel, and D2EHPA (di-(2-ethylhexyl)phosphoric acid) for the recovery of zinc. In these modules the flow pattern of both feed and stripping solutions is plug flow, which led to very high recovery of metal ions. For example, 99.97% of cobalt in the feed was recovered in a once-through operation, and cobalt could be pumped against its concentration gradient even if the ratio of the metal concentration in the strip phase to that in the feed phase was as high as 70,000. It was confirmed by a life test of the module that the membrane was stable for more than one month without appreciable decrease in metal flux, and that the degraded membrane could be easily and rapidly regenerated without interrupting the permeation of metal ions by re-impregnating the module with the organic membrane solution. The degree of removal for both single and simultaneous permeation of cobalt and nickel was satisfactorily simulated by design equations of the module and the flux equations in which the formation of aggregates of metal-carrier complexes was taken into account.

*To whom correspondence should be addressed.

INTRODUCTION

The separation technique using liquid membranes has been noted as an attractive method for the separation and concentration of various substances such as metal ions, acids, bases, and organic compounds (*1*). One of the liquid membrane configurations that can be used for practical purposes is supported liquid membranes. In this type of liquid membrane the operation is very simple compared to emulsion-type liquid membranes which need the breaking of emulsions to recover the concentrated solution and membrane solution for reuse.

There are several problems which must be solved in order to use supported liquid membranes commercially. One of the important problems is to develop membrane modules which satisfy the following conditions.

(1) High degree of recovery can be attained.
(2) Membrane life-time is long.
(3) Even if the membrane is degraded, it can be easily regenerated by simple operations without interrupting the permeation of the solutes.
(4) The flow patterns of both feed and strip phases are well defined so that the characteristics of the module such as permeability and degree of recovery may be easily analyzed.
(5) The design and the scale-up of the module are easy.

The supported liquid membrane can be made into such modules as a plate-and-frame multicompartment cell, a hollow fiber assembly, or a spiral-type module. It has been generally recognized that in view of membrane area to volume ratio, S/V, the hollow fiber module is more favorable than other types of modules. Therefore, special attention has been paid to this type of module (*2–5*). However, it seems impossible to use hollow fibers of very small diameter because clogging may occur. Therefore, the membrane area to volume ratio of other types of modules are comparable to the hollow fiber module.

The spiral-type module has a high S/V value which depends mainly on the thickness of the spacer inserted in the channels. For example, if the thickness is 1 mm, then S/V may be about 1000 m^2/m^3. Moreover, since the flow pattern of the feed and strip phases is approximated as plug flow, high recovery of permeates is expected, which is in contrast with the hollow fiber module where the fluid on the shell side moves in a complicated flow pattern.

In the present study, spiral-type supported liquid membrane modules

were developed, and the single permeation of cobalt, nickel, and zinc, and the simultaneous permeation of cobalt and nickel, were carried out using these modules. The carriers used were PC-88A (active species: 2-ethylhexylphosphonic acid mono-2-ethylhexyl ester, EHPNA) for cobalt and nickel permeation, and D2EHPA (di-2-ethylhexylphosphoric acid) for the recovery of zinc. The degree of recovery and the selectivity in these transport systems were analyzed using design equations representing differential mass balances of permeates and flux equations in which the formation of the aggregates of metal–carrier complexes were taken into account.

It is shown that this type of module is stable more than one month, and also that the modules can be easily and rapidly regenerated by re-impregnating them with organic membrane solutions without interrupting the permeation of metal ions.

EXPERIMENTAL

As a support of immobilized liquid membranes, microporous polypropylene film, Duragard 2502, supplied from Polyplastics Co., was used. This film is produced by sticking two sheets of Duragard 2500 (thickness, 25 μm; porosity, 0.47; pore size, 0.04 × 0.4 μm) together without using an adhesive. The width of the sheet is 30.5 cm. A schematic diagram of the module is shown in Fig. 1. The support films and polyester mesh spacers (thickness, 1.1 mm) were spirally wound around the tubes through which feed and strip solutions were supplied, and the outer surface of the module was sealed with an adhesive of the epoxy type. The raffinate and strip solutions were withdrawn through outlet tubes inserted in the outermost channels. Modules with different lengths of the support film were produced, i.e., Module A (total membrane length: about 1.6 m, channel length of feed and strip side: about 0.8 m, diameter of module: 6.5 cm) and Module B (total membrane length: about 4 m, channel length: about 2 m, diameter of module: 10 cm).

The organic membrane solutions were prepared by dissolving PC-88A in *n*-dodecane for the permeation of cobalt and nickel, and D2EHPA for the recovery of zinc. The modules were impregnated with the organic membrane solutions by passing them through the channels of the strip phase, and then the excess of the organic solution was removed by flowing deionized water in the channel. The module was operated in a once-through mode for the feed solution. With respect to the strip solution, a recycling mode was used in the single permeation of cobalt, nickel, and zinc, and a once-through mode was used for the simultaneous

permeation of cobalt and nickel. The feed and strip solutions were supplied at approximately the same flow rate by a tubing pump. After every permeation experiment the module was washed with ethanol, and subsequently with heptane, by passing them through the channels of the feed and strip sides. Then the module was dried with air.

The feed solutions were prepared by dissolving nitrates of metals in deionized water. In the experiment for the recovery of cobalt and nickel, acetic acid–sodium acetate buffer solutions were used. Sulfuric acid (2 mol/dm^3) was used as the strip solution. The volume of the strip solution was 2 dm^3 in a recycling operation. The metal concentrations were determined by an atomic absorption spectrophotometer. The temperature was 25°C.

DESIGN EQUATIONS OF MODULE

(1) Extraction Equilibria

It has already been found by the present authors (*6*) that the equilibria in the extraction of cobalt and nickel with PC-88A can be expressed as follows.

Dimerization of the extractant $\overline{HL}$ in the organic phase is expressed by

$$2\overline{HL} \rightleftharpoons (\overline{HL})_2$$

$$K_2 = [(\overline{HL})_2]/[\overline{HL}]^2 \tag{1}$$

The extraction equilibria of cobalt, nickel, and sodium at low loading ratio are expressed by

$$Co^{2+} + 2(\overline{HL})_2 \rightleftharpoons \overline{CoL_2(HL)_2} + 2H^+$$

$$K_{exCo} = (\overline{[CoL_2(HL)_2]}[H^+]^2/[Co^{2+}][(\overline{HL})_2]^2)_{eq} \tag{2}$$

$$Ni^{2+} + 3(\overline{HL})_2 \rightleftharpoons \overline{NiL_2(HL)_4} + 2H^+$$

$$K_{exNi} = (\overline{[NiL_2(HL)_4]}[H^+]^2/[Ni^{2+}][(\overline{HL})_2]^3)_{eq} \tag{3}$$

$$Na^+ + 2(\overline{HL})_2 \rightleftharpoons \overline{NaL(HL)_3} + H^+$$

$$K_{exNa} = (\overline{[NaL(HL)_3]}[H^+]/[Na^+][(\overline{HL})_2]^2)_{eq} \tag{4}$$

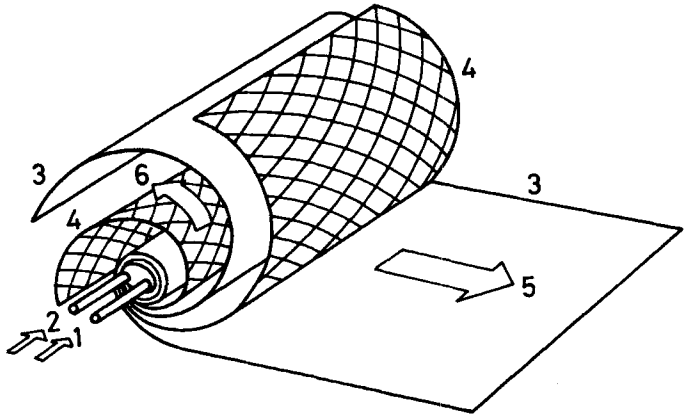

FIG. 1. Schematic diagram of spiral-type supported liquid membrane module. (1) Inlet of feed solution, (2) inlet of strip solution, (3) liquid membrane, (4) spacer, (5) feed solution, (6) strip solution.

Here $\overline{HL}$ and $(\overline{HL})_2$ are the monomer and the dimer of the extractant, respectively, and the bars denote the species in the organic phase. The extraction equilibrium of sodium was considered because acetic acid-sodium acetate buffer solutions were used in the permeation experiments. Equations (1)-(4) are the same as those reported by Komasawa et al. (*7*).

It was found by gel permeation chromatography and vapor pressure osmometry that at high metal loading, aggregates of metal-extractant complexes are formed which contain 3-10 molecules of $(\overline{HL})_2$ on the average. For simplicity, it was assumed that the aggregates consist of equimolar metal and $(\overline{HL})_2$ regardless of the metal loading, and that the aggregates can be expressed as $(\overline{ML_2})_n$, where M denotes cobalt or nickel. The concentrations of $\overline{CoL_2}$ and $\overline{NiL_2}$ were found to be expressed by the following empirical equations (*6*):

$$[\overline{CoL_2}] = K_{Cop}[\overline{CoL_2(HL)_2}]^{1.57}[(\overline{HL})_2]^{-0.802} \quad (5)$$

$$[\overline{NiL_2}] = K_{NiP}[\overline{NiL_2(HL)_4}]^{0.836}[(\overline{HL})_2]^{-0.750} \quad (6)$$

Here, $[ML_2]$ is the concentration of the aggregate expressed in mol of metal/dm^3.

The conservation of the extractant is represented by

$$[(\overline{HL})_2]_0 = [\overline{HL}]/2 + [(\overline{HL})_2] + 2[\overline{CoL_2(HL)_2}] + 3[\overline{NiL_2(HL)_4}] + [\overline{CoL_2}] + [\overline{NiL_2}] + 2[\overline{NaL(HL)_3}] \quad (7)$$

where $[(HL)_2]_0$ is the total concentration of the carrier. As shown by the solid lines in Figs. 2 and 3, the distribution ratios (ratio of metal concentration in the organic phase to that in the aqueous phase) of cobalt and nickel were satisfactorily predicted by Eqs. (1)-(3) and (5)-(7) for the cases of single extraction and of simultaneous extraction. Distribution ratios computed without taking into account the formation of aggregates are shown by the broken lines in these figures, which are much lower than the experimental data at high metal loading, i.e., at low $[H^+]$.

The equilibria in the extraction of zinc with D2EHPA were found to be expressed by

$$Zn^{2+} + 1.5(\overline{HL})_2 \rightleftharpoons \overline{ZnL_2(HL)} + 2H^+$$

$$K_{exZn} = [\overline{ZnL_2(HL)}][H^+]^2/[Zn^{2+}][(\overline{HL})_2]^{1.5} \quad (8)$$

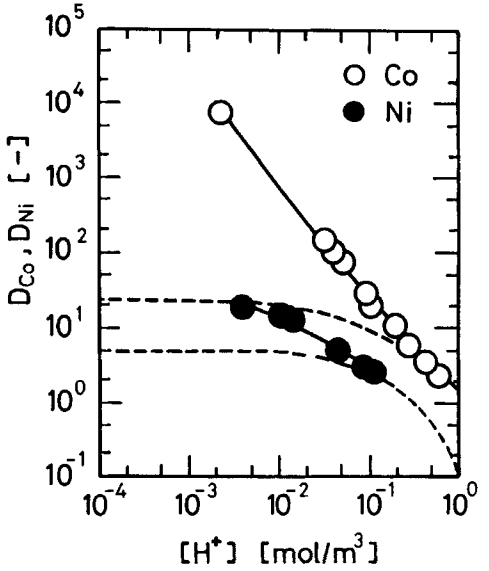

FIG. 2. Distribution ratios of Co and Ni in the single extraction. $[(\overline{HL}_2]_0 = 0.735$ mol/dm^3; $[Co]_0 = [Ni]_0 = 0.085$ mol/dm^3; volume ratio, $V_{aq}/V_{org} = 5$. Buffer solutions were not used.

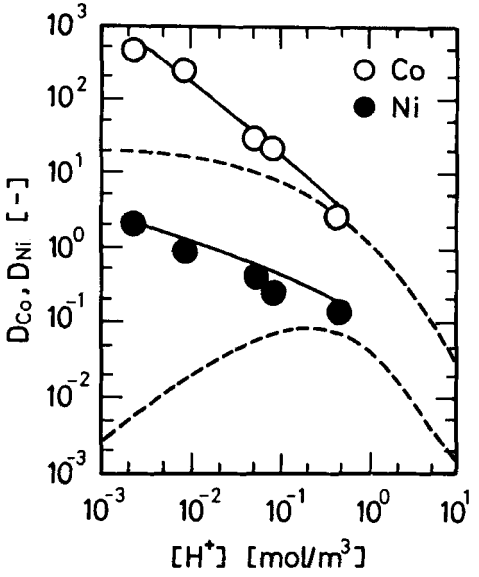

FIG. 3. Distribution ratios of Co and Ni in simultaneous extraction. Conditions are the same as in Fig. 2.

Extraction of sodium with D2EHPA is expressed by Eq. (4) (*12*).

(2) Model of the Permeation of Metals through Supported Liquid Membranes

(a) Permeation of Cobalt and Nickel

The permeation of metals through supported liquid membranes consists of many elementary steps (*8*). Here, the diffusion of metal ions through aqueous boundary layer present at the feed solution-membrane interface, instantaneous distribution of metals at the feed-membrane interface, and the diffusion of the carrier and the complexes in the liquid membrane were considered because the resistances of other steps were found to be negligibly small. The diffusion of hydrogen ion in the feed phase is also ignored because buffer solutions were used. The concentration profiles are shown in Fig. 4. The fluxes are expressed as follows (6).

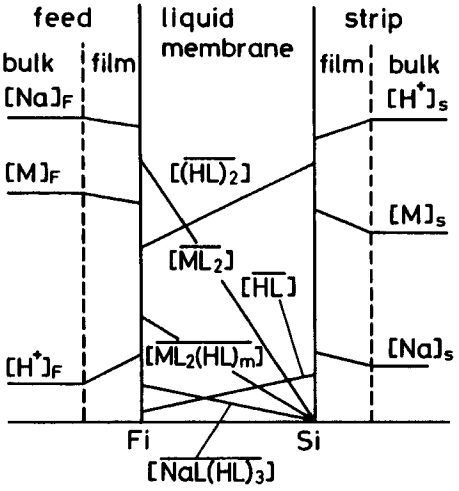

FIG. 4. Model of permeation of metal ions.

$$J_{Co} = k_{FCo}([Co]_F - [Co]_{Fi}) = k_{mCo}[\overline{CoL_2(HL)_2}]_{Fi} + k_{mCoP}[\overline{CoL_2}]_{Fi} \quad (9)$$

$$J_{Ni} = k_{FNi}([Ni]_F - [Ni]_{Fi}) = k_{mNi}[\overline{NiL_2(HL)_4}]_{Fi} + k_{mNiP}[NiL_2]_{Fi} \quad (10)$$

$$J_{Na} = k_{FNa}([Na]_F - [Na]_{Fi}) = k_{mNa}[\overline{NaL(HL)_3}]_{Fi} \quad (11)$$

The continuity of the total flux of the carrier is expressed by

$$k_{mB}([\overline{(HL)_2}]_{Si} - [\overline{(HL)_2}]_{Fi}) + 0.5k_{mB'}([\overline{HL}]_{Si} - [\overline{HL}]_{Fi})$$
$$= 2k_{mCo}[\overline{CoR_2(HL)_2}]_{Fi} + k_{mCoP}[\overline{CoL_2}]_{Fi} + 3k_{mCo}[\overline{NiR_2(HL)_4}]_{Fi}$$
$$+ k_{mNiP}[\overline{NiL_2}]_{Fi} + 2k_{mNa}[\overline{NaL(HL)_3}]_{Fi} \quad (12)$$

where k_F and k_m are the mass transfer coefficients in the boundary layer of the feed solution and that in the liquid membrane, respectively, and subscripts B, B′, CoP, NiP, F, S, and i denote $(HL)_2$, HL, CoL_2, NiL_2, the feed phase, the strip phase, and the interface, respectively. The conservation of the carrier in the membrane is approximately expressed by

$$[\overline{(HL)_2}]_0 L = \int_0^L ([\overline{HL}]/2 + [\overline{(HL)_2}] + 2[\overline{CoL_2(HL)_2}] + 3[\overline{NiL_2(HL)_4}] + 2[\overline{NaL(HL)_3}] + [\overline{CoL_2}] + [\overline{NiL_2}])dx \quad (13)$$

where $[\overline{(HL)_2}]_0$ is the initial concentration of the carrier evaluated on the assumption that all the carrier exists in its dimeric form. The 12 unknown interfacial concentrations can be determined using the above equations by the trial-and-error procedure on the assumption that extraction equilibria were established at the feed–membrane interface, and the concentrations of the complexes are zero at the strip–membrane interface. Then, the flux of each metal ion can be calculated. Here, the complexation between metal ion and acetate ion was also considered. The concentration of free metal ion is expressed by

$$[M^{2+}] = [M]/\{1 + \beta_{1M}[OAc^-] + \beta_{2M}[OAc^-]^2\} \quad (M = Co, Ni) \quad (14)$$

where [M] denotes the total concentration of cobalt or nickel, and β_{iM} is the stability constant of the complex formation $M^{2+} + iOAc^- \rightleftharpoons M(OAc^-)_i^{2-i}$. It was experimentally confirmed that the present permeation model could simulate the single as well as the simultaneous permeation rates of cobalt and nickel fairly well even when the metal loading at the feed–membrane interface was very high (*6*). Figures 5 and 6 show typical examples of the comparison between the experimentally observed permeation rates of cobalt and nickel with the computed permeation rates on the basis of the present permeation model.

(b) Permeation of Zinc

Because most of the experiments were performed under the condition of low loading ratio, the formation of the aggregates of the metal-D2EHPA complex was not considered. The permeation rates of zinc and sodium are calculated by the following equations.

$$J_{Zn} = k_{FZn}([Zn]_F - [Zn]_{Fi}) = k_{mZn}[\overline{ZnL_2(HL)}]_{Fi} \quad (15)$$

$$J_{Na} = k_{FNa}([Na]_F - [Na]_{Fi}) = k_{mNa}[\overline{NaL(HL)_3}]_{Fi} \quad (16)$$

$$J_H = k_{FH}([H^+]_F - [H^+]_{Fi}) = -2J_{Zn} - J_{Na} \quad (17)$$

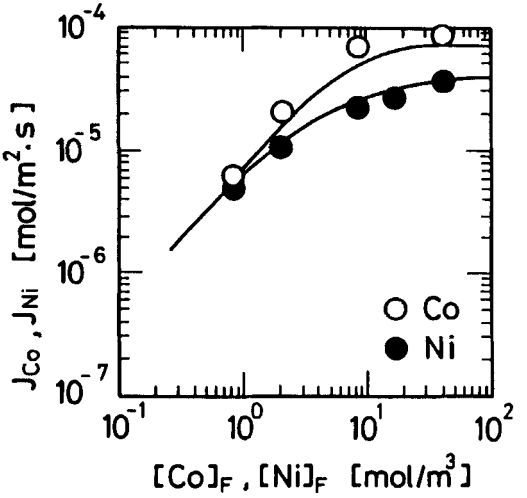

FIG. 5. Effect of metal concentration in the feed phase on J_{Co} and J_{Ni} in the single permeation. $[\overline{(HL_2)}]_0 = 0.735$ mol/dm^3, $[H^+] = 1 \times 10^{-5}$ mol/dm^3, support of membrane: FP-010 (microporous membrane made of Teflon).

$$k_B([\overline{HL})_2]_{Si} - [\overline{(HL)_2}]_{Fi}) + 0.5k_{B'}([\overline{HL}]_{Si} - [\overline{HL}]_{Fi})$$
$$= 1.5k_{mZn}[\overline{ZnL_2(HL)}]_{Fi} + 2k_{mNa}[\overline{NaL(HL)_3}]_{Fi} \quad (18)$$

$$[\overline{(HL)_2}]_0 L = \int_L^0 ([\overline{HL}]/2 + [\overline{(HL)_2}] + 1.5[\overline{ZnL_2(HL)}]$$
$$+ 2[\overline{NaL(HL)_3}])dx \quad (19)$$

(c) Permeation Rates for Special Conditions

Simple flux equations can be obtained in the following cases.

Case 1. When metal concentration is low and the distribution ratio of the metal at the feed-membrane interface is sufficiently high, i.e., when pH and carrier concentration are high, the diffusion of metal species through the boundary layer in the feed phase is rate-controlling. Then J_M is expressed by Eq. (20) (*6*, *8*):

$$J_M = k_{FM}[M]_F \quad (20)$$

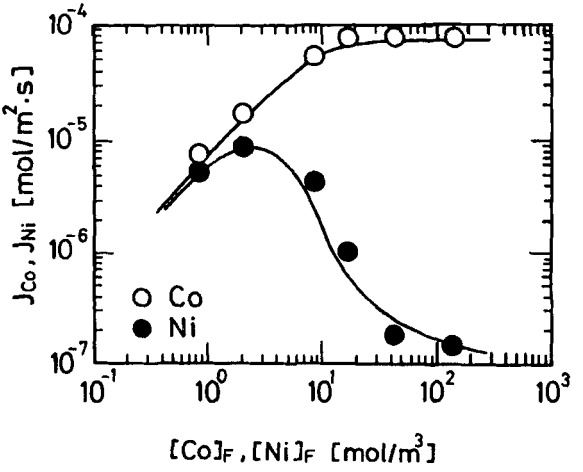

FIG. 6. Effect of metal concentration in the feed phase on J_{Co} and J_{Ni} in the simultaneous permeation. Conditions are the same as in Fig. 5.

This equation is applicable to the region of low metal concentration in Figs. 5 and 6.

Case 2. When metal concentration is high and the distribution ratio is also high, the carrier at the feed-membrane interface is exhausted by complexation with the metal ion. In this case the diffusion of the carrier from the strip-membrane to the feed-membrane interface is rate-controlling, and J_M becomes maximum.

$$J_M = J_{Mmax} \tag{21}$$

This value depends on the metal species, the carrier concentration, and the degree of polymerization of the metal-carrier complex, and can be experimentally measured using a regular transfer cell (*6*). These values are shown in Table 1 for the permeation systems studied. Equation (21) holds in the region of high metal concentration for the permeation of cobalt in Figs. 5 and 6.

Case 3. If the distribution of metal at the feed-membrane interface is low, the diffusion of the complex in the liquid membrane is rate-determining. Then the permeation rate is expressed by

TABLE 1
Maximum Fluxes of Metal Ions Measured under the Condition That Diffusion of Carrier in the Liquid Membrane Is Rate-Controlling

Metal	Carrier	Diluent	$[(\overline{HL})_2]_0$ (mol/dm^3)	$[M]_F$ (ppm)	pH_F	J_{max} (mol/(m^2·s))
Cobalt	PC-88A	*n*-Dodecane	0.735	5040	5.95	6.84×10^{-5}
Cobalt	PC-88A	*n*-Dodecane	0.294	4630	6.0	7.22×10^{-5}
Cobalt	PC-88A	Dispersol	0.735	2500	5.8	7.07×10^{-5}
Nickel	PC-88A	*n*-Dodecane	0.735	5270	5.65	3.66×10^{-5}
Zinc	D2EPHA	*n*-Dodecane	0.698	4750	4.0	9.37×10^{-5}

$$J_M = k_{mM}[M]_{Fi} \tag{22}$$

where $[M]_{Fi}$ is the concentration of the metal-carrier complex formed at low loading ratio. This concentration can be expressed by the extraction equilibrium using the bulk concentrations in the feed solutions and $[(\overline{HL})_2]_0$.

(3) Design Equations of Spiral-Type Module

If the flow pattern of both the feed and the strip phase is assumed to be plug flow as shown in Fig. 7, the following design equations representing differential mass balances of metal ions are obtained.

$$d[Co]_F/ds = -J_{Co}/v_F \tag{23a}$$

$$d[Ni]_F/ds = -J_{Ni}/v_F \tag{23b}$$

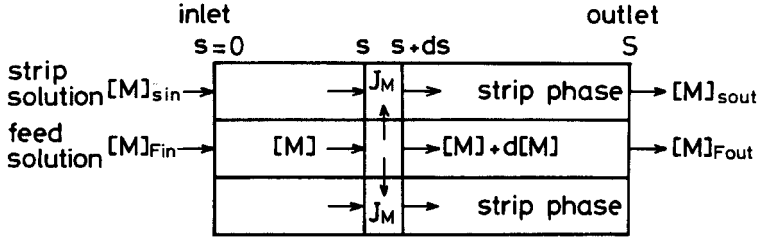

FIG. 7. Differential material balances of permeates in the module.

$$d[\mathrm{Zn}]_F/ds = -J_{\mathrm{Zn}}/v_F \tag{23c}$$

$$d[\mathrm{Na}]_F/ds = -J_{\mathrm{Na}}/v_F \tag{23d}$$

The boundary condition is expressed by

$$s = 0; \qquad [\mathrm{M}]_F = [\mathrm{M}]_{F\mathrm{in}} \qquad (\mathrm{M} = \mathrm{Co, Ni, Zn, Na}) \tag{24}$$

Here, s is the membrane area and v_F is the volumetric flow rate of the aqueous feed solution. Because J_{M} can be evaluated for given values of $[\mathrm{M}]_F$ as described above, Eq. (23) can be integrated numerically to give $[\mathrm{M}]_{F\mathrm{out}}$. For the permeation of cobalt and nickel, Eqs. (23a), (23b), and (23d) were simultaneously integrated. Here, hydrogen ion concentration in the feed, $[\mathrm{H}^+]_F$, was calculated by taking account of Eq. (25) and the ionic equilibria in acetic acid–sodium acetate buffer solution:

$$J_{\mathrm{H}} = -2(J_{\mathrm{Co}} + J_{\mathrm{Ni}}) - J_{\mathrm{Na}} \tag{25}$$

In the case of zinc permeation where sodium nitrate was added to adjust ionic strength and no buffer solution was used, Eqs. (23c), (23d), and the following equation were simultaneously solved:

$$d[\mathrm{H}^+]_F/ds = -J_{\mathrm{H}}/v_F \tag{26}$$

The equations for $[\mathrm{M}]_{F\mathrm{out}}$ for the single permeation can be derived for each case described above.

Case 1. From Eqs. (20), (23), and (24), the following equation is derived:

$$[\mathrm{M}]_{F\mathrm{out}}/[\mathrm{M}]_{F\mathrm{in}} = \exp(-k_{F\mathrm{M}}S/v_F) \tag{27}$$

Case 2. From Eqs. (21), (23), and (24), Eq. (28) is obtained:

$$[\mathrm{M}]_{F\mathrm{out}} = [\mathrm{M}]_{F\mathrm{in}} - J_{\mathrm{Mmax}}S/v_F \tag{28}$$

Case 3. For example, the outlet concentration of cobalt is derived from Eqs. (2), (14), and (22)–(24) by assuming that $[\mathrm{H}^+]_F$ is constant.

$$[\mathrm{Co}]_{F\mathrm{out}}/[\mathrm{Co}]_{F\mathrm{in}} = \exp(-K^{\mathrm{app}}_{\mathrm{exCo}}k_{m\mathrm{Co}}[(\overline{\mathrm{HL}})_2]_0^2S/[\mathrm{H}^+]_F^2v_F) \tag{29}$$

$$K^{\mathrm{app}}_{\mathrm{exCo}} = K_{\mathrm{exCo}}/\{1 + \beta_{1\mathrm{Co}}[\mathrm{OAc}^-] + \beta_{2\mathrm{Co}}[\mathrm{OAc}^-]^2\} \tag{30}$$

RESULTS AND DISCUSSION

The module can be operated either with countercurrent flow or cocurrent flow of the feed and strip solutions. Here, all runs were carried out with cocurrent flow because there is no difference in the overall driving forces of metal transports between these operations.

(1) Single Permeation of Cobalt and Nickel

The experiments were performed in a once-through mode for the feed solution and the recycling mode for the strip solution. Figure 8 shows the effect of the flow rate of the feed solution on $[Co]_{Fout}/[Co]_{Fin}$. These data were obtained with Module B whose total membrane length was about 4 m. In this experiment, Dispersol, a sort of kerosene consisting mainly of naphthenic hydrocarbon, was used as a diluent, while *n*-dodecane was used in other experiments. Although not shown in Fig. 8, it was found that when $[Co]_{Fin}$ was low, i.e., 100 ppm, $[Co]_{Fout}$ was so low that it could

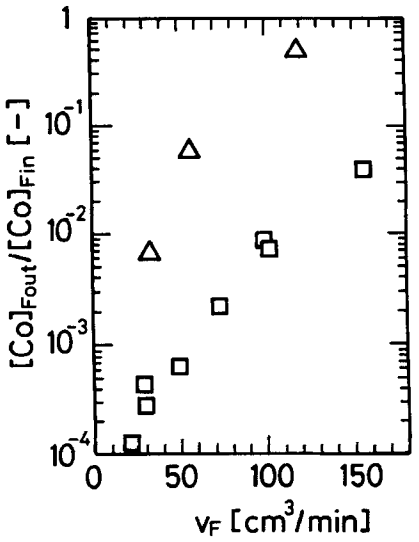

FIG. 8. Recovery of cobalt by Module B. $[(\overline{HL})_2]_0 = 0.735$ mol/dm^3, $pH_{Fin} = 5.60$, $S = 0.72$ m^2, diluent: Dispersol. (□) $[Co]_{Fin} = 1000$ ppm, $[CH_3COOH]_F + [CH_3COONa]_F = 0.2$ mol/dm^3. (△) $[Co]_{Fin} = 2990$ ppm, $[CH_3COOH]_F + [CH_3COONa]_F = 0.5$ mol/dm^3. $CoSO_4$ was used instead of $Co(NO_3)_2$.

not be measured accurately by an atomic absorption spectrophotometer. $[Co]_{Fout}$ might be as low as 0.01 ppm, and the recovery was about 99.99%. It should be noted that such high recovery has never been reported. The cause of such high recovery is that at low cobalt concentration, diffusion of cobalt in the feed phase limits the permeation rate and the resistance in the membrane can be neglected. Another important cause is that the flow pattern of the feed phase is approximately plug flow. Compared to complete mixing flow, plug flow is favorable in obtaining high recovery in a once-through mode, especially when $[M]_{Fout}$ must be decreased to the very low concentration level where J_M is proportional to $[M]_F$ as expressed by Eq. (20) (*5*). Therefore, this type of module is useful for the recovery or removal of heavy metal ions from their dilute solutions as encountered in wastewater treatments. It may also be possible to use hollow fiber modules where the feed solution flows inside the hollow fibers.

When $[M]_{Fin}$ was relatively high, i.e., 1000 ppm, and v_F was low, 99.97% of cobalt was successfully recovered. In this run, $[Co]_s$, the concentration of cobalt in the strip solution, was 8130 ppm. Therefore, it was demonstrated that cobalt could be pumped against its concentration gradient even when $[Co]_s$ was about 70,000 times as high as $[Co]_{Fout}$.

When $[Co]_{Fin}$ is sufficiently high, the transport of cobalt is limited by the diffusion of the carrier in the membrane, and J_{Co} approaches J_{Comax}. The values of J_{Comax} measured by the usual two-compartment cell are shown in Table 1 together with the values for other metals. Using the data obtained at $[Co]_{Fin}$ = 2990 ppm, the effective membrane area was calculated as 0.72 m^2, which is about 60% of the total area of the membrane used for producing the module (width: 0.305 m, length: 4 m, area: 1.22 m^2). The decrease in effective membrane area is mainly due to blocking of the membrane surface by the spacer and by the adhesive used to seal the sides of the modules. Such a decrease in effective membrane area, however, may also occur in the case of hollow fiber modules.

Figure 9 shows the data obtained with Module A with a total membrane length of about 1.6 m. The effective membrane area was determined from the data obtained at $[Co]_{Fin}$ = 4780 ppm using Eq. (28), and is plotted against v_F in Fig. 10. It can be seen that S is almost constant regardless of v_F.

When $[Co]_{Fin}$ is low, i.e., 101 ppm, the diffusion of cobalt through the boundary layer in the feed phase limits the permeation rate. Then Eq. (27) is applicable. Using this equation, the mass transfer coefficient of cobalt in the feed phase, k_{FCo}, was calculated, and it is plotted against v_F in Fig. 11, which indicates that k_{FCo} is proportional to $v_F^{0.5}$. The exponent n in the relation of $k_F \propto v_F^n$ ranges from 0 to 1/3 for the hollow fiber module in which the feed solution flows inside the hollow fibers in laminar flow

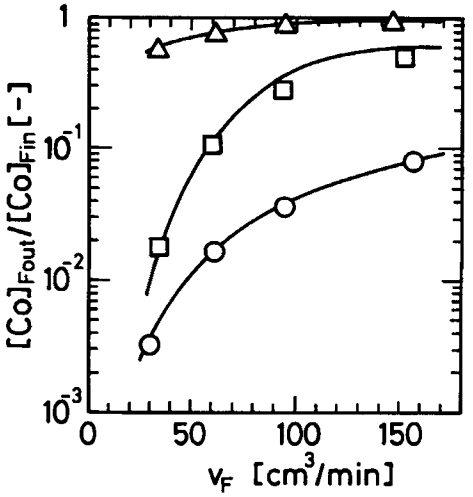

FIG. 9. Recovery of cobalt by Module A. $[(\overline{HL})_2]_0 = 0.735$ mol/dm^3, $pH_{Fin} = 5.96$. (△) $[Co]_{Fin} = 4780$ ppm, $[CH_3COOH]_F + [CH_3COONa]_F = 0.5$ mol/dm^3. (□) $[Co]_{Fin} = 990$ ppm, $[CH_3COOH]_F + [CH_3COONa]_F = 0.2$ mol/dm^3. (○) $[Co]_{Fin} = 101$ ppm, $[CH_3COOH]_F + [CH_3COONa]_F = 0.1$ mol/dm^3.

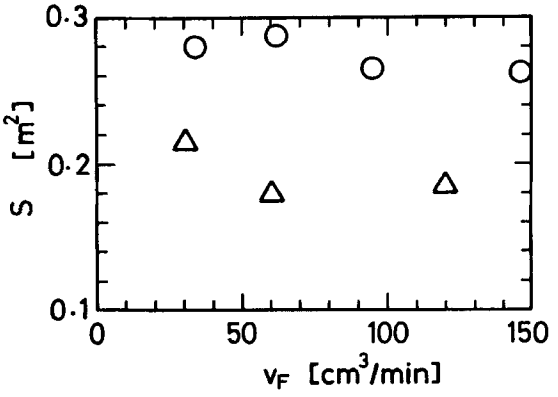

FIG. 10. Effective membrane area. (○) S in the experiment on the permeation of cobalt. (△) S in the experiment on the permeation of nickel. Experimental conditions as given in Figs. 8 and 13.

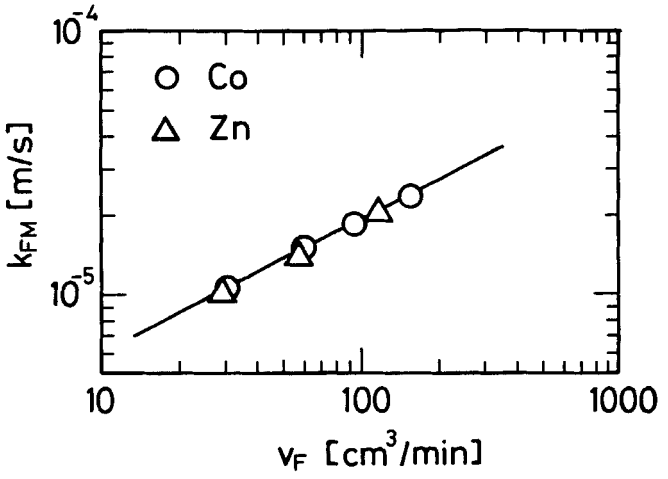

FIG. 11. Mass transfer coefficients of cobalt and zinc in the feed phase.

(9). Therefore, the dependency of v_F on k_F for spiral-type modules is stronger than that for hollow fiber modules. This suggests that the extent of the decrease in the recovery with an increase in v_F is less for spiral-type modules than for hollow-fiber modules and also that the spiral-type module is favorable for the treatment of a large amount of feed solution. Plate-and-frame type modules may have the same characteristics as spiral-type modules.

When a feed solution flows inside a hollow fiber, the average mass transfer coefficient k_F is expressed by the following equation (9):

$$\mathrm{Sh}_m = 3.66 + \frac{0.0668(lD/d^2u)^{-1}}{1 + 0.04(lD/d^2u)^{-2/3}} \tag{31}$$

where $\mathrm{Sh}_m = k_F d/D$. The values of k_F were calculated by Eq. (31) using a typical value of the diffusivity of a metal ion and the dimensions of a hollow fiber, and are shown as a function of u, the average velocity of the feed solution in Fig. 12 where the data of Fig. 11 are also shown by a solid line. It can be seen that when u is larger or when d is large, k_F in the spiral-type module is larger than that in a hollow fiber due to the turbulence caused by the spacer. From a practical viewpoint, it seems undesirable to use fibers of too small a diameter because the pressure drop becomes high as shown in Fig. 12 and also because clogging may make the operation impossible.

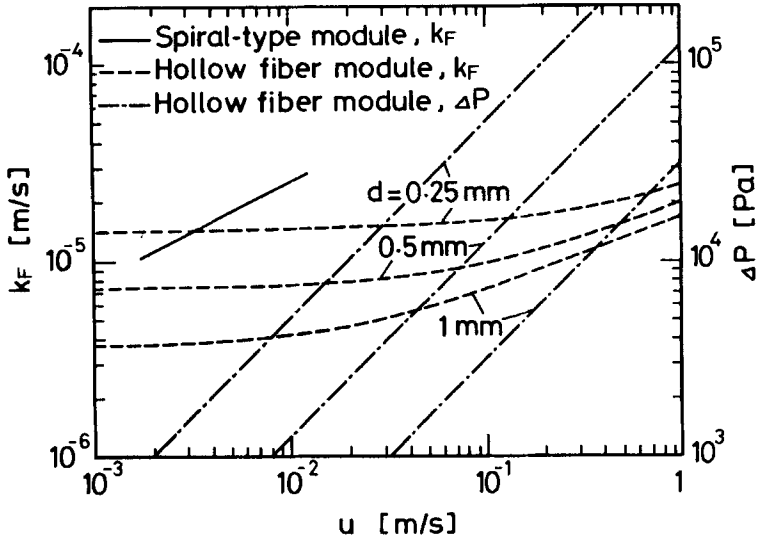

FIG. 12. Comparison of mass transfer coefficient through the boundary layer of feed solution in spiral-type Module A with that in hollow fiber modules. k_F and ΔP for hollow fiber modules were calculated by Eq. (31) and the Hagen-Poiseulle equation, respectively. Length of hollow fiber = 1 m, viscosity of feed solution = 1×10^{-3} Pa · s, diffusivity of metal ion in the feed solution = 1×10^{-9} m^2/s.

When $[Co]_{Fin}$ was 990 ppm, $[Co]_{Fout}$ was less than 100 ppm at a low feed rate. In this case a transition of the rate-controlling step from the diffusion in the membrane to that in the feed phase occurs at a certain position of the module.

The result on the recovery of nickel is shown in Fig. 13. S was calculated by a similar procedure, and it is shown in Fig. 10. S is considerably less than that determined from the recovery of cobalt, probably due to incomplete absorption of the organic membrane solution in the micropores of the polymer supports. It is seen from a comparison of Figs. 9 and 13 that the removal of nickel is less than that of cobalt because of lower values of S and the distribution ratio.

(2) Simultaneous Permeation of Cobalt and Nickel

The experiments were carried out in a once-through mode both for the feed and strip solutions. Figures 14 and 15 show the effect of metal concentration in the simultaneous permeation of cobalt and nickel. Since

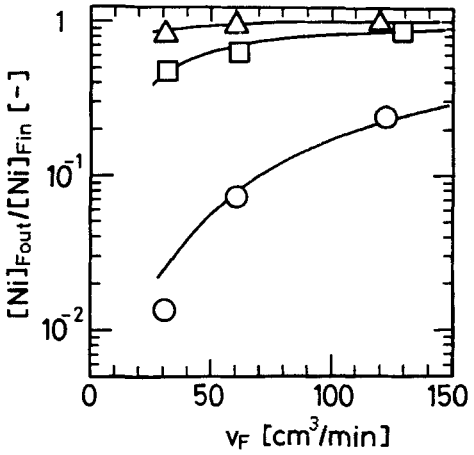

FIG. 13. Recovery of nickel by module. $[\overline{(HL)_2}]_0 = 0.735$ mol/dm^3, $pH_{Fin} = 5.62$. (△) $[Ni]_{Fin} = 5280$ ppm, $[CH_3COOH]_F + [CH_3COONa]_F = 0.5$ mol/dm^3. (□) $[Ni]_{Fin} = 988$ ppm, $[CH_3COOH]_F + [CH_3COONa]_F = 0.2$ mol/dm^3. (○) $[Ni]_{Fin} = 94.5$ ppm, $[CH_3COOH]_F + [CH_3COONa]_F = 0.1$ mol/dm^3.

the distribution ratio of cobalt is larger than that of nickel, it is expected that cobalt is selectively transported through the membrane over nickel. This is true especially when the metal concentration is so high that the mass transfer resistance in the feed phase can be neglected and the diffusional resistance in the liquid membrane is rate-determining. On the other hand, when $[M]_{Fin}$ is as low as 100 ppm, the transports of both cobalt and nickel are limited by the diffusion in the feed phase. Because there is little difference in k_{FCo} and k_{FNi}, highly selective transport of cobalt over nickel is not expected, in agreement with the experimental results.

(3) Recovery of Zinc

In experiments on the recovery of cobalt and nickel, buffer solutions were used to maintain the pH of the feed solution at a high value. If buffer solutions are not used, the pH of the feed solution decreases as the feed solution passes through the channel, and the permeation essentially stops at some position of the module. This means that all the membrane in the module is not used for permeation.

From a practical point of view, it is undesirable to use buffer solutions.

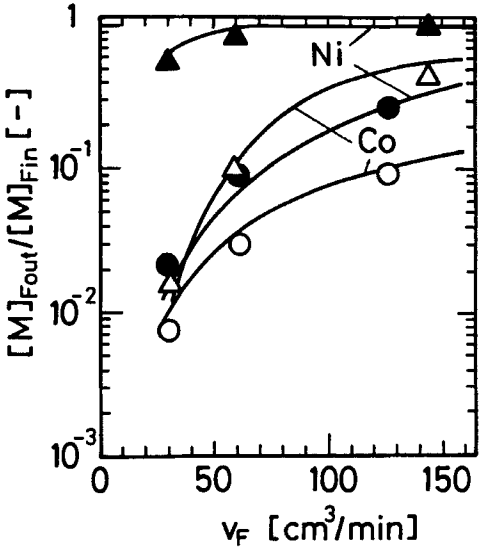

FIG. 14. Simultaneous permeation of cobalt and nickel by Module A. $[(\overline{HL})_2]_0$ = 0.735 mol/dm^3, pH_{Fin} = 5.96. (△, ▲) $[Co]_{Fin}$ = $[Ni]_{Fin}$ = 1000 ppm, $[CH_3COOH]_F$ + $[CH_3COONa]_F$ = 0.2 mol/dm^3, S = 0.292 m^2. (○, ●) $[Co]_{Fin}$ = 99 ppm, $[Ni]_{Fin}$ = 103 ppm, $[CH_3COOH]_F$ + $[CH_3COONa]_F$ = 0.1 mol/dm^3, S = 0.223 m^2.

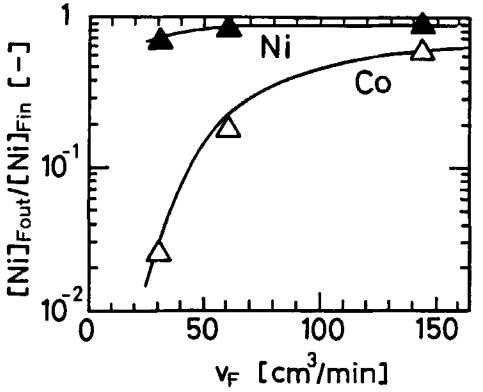

FIG. 15. Simultaneous permeation of cobalt and nickel by Module A. $[(\overline{HL})_2]_0$ = 0.294 mol/dm^3, pH_{Fin} = 5.98, $[Co]_{Fin}$ = 960 ppm, $[Ni]_{Fin}$ = 1000 ppm, $[CH_3COOH]_F$ + $[CH_3COONa]_F$ = 0.2 mol/dm^3, S = 0.229 m^2.

The recovery of zinc from acidic aqueous solutions is an example where metal can be transported without using buffer solution or the pH of the feed solution in the module can be maintained almost constant.

It is also important to know the stability of the membrane and to find a method for regenerating degraded membranes. For these purposes, experiments on the recovery of zinc were carried out. D2EHPA was used as the carrier because D2EHPA can extract zinc from more acidic solutions than EHPNA, which is favorable because the relative increase in the hydrogen ion concentration caused by zinc permeation is smaller.

Figure 16 shows a plot of $[Zn]_{Fout}$ vs v_F under the condition that the diffusion of zinc in the feed phase is rate-determining. Although the pH of the feed solution decreased from 5.58 to about 2.5, about 99.2% of the zinc was successfully recovered at $v_F = 30$ cm^3/min. Using Eq. (28), the effective membrane area was determined as 0.242 m^2 in an experiment carried out at high $[Zn]_{Fin}$, and k_{FZn} was calculated by Eq. (27) for each value of v_F. As shown in Fig. 11, the values of k_{FZn} agree with those of k_{FCo}.

Figure 17 shows the result of the life test of the module. Since $[Zn]_{Fin}$ was low, the diffusion in the feed phase was considered to be rate-

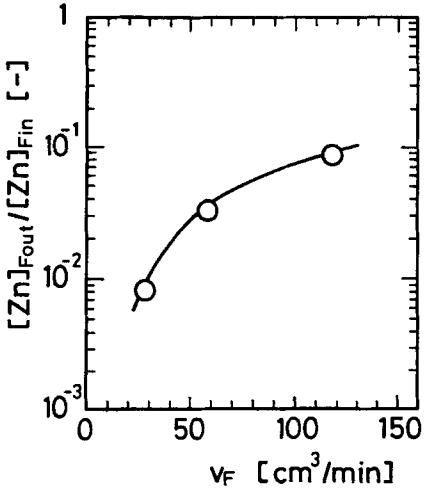

FIG. 16. Recovery of zinc by Module A. Carrier, D2EHPA; diluent, *n*-dodecane; $[(\overline{HL})_2]_0 = 0.698$ mol/dm^3, $pH_{Fin} = 5.58$, $pH_{Fout} = 2.5$, $[Zn]_{Fin} = 100$ ppm, $I = 0.2$ mol/dm^3, $S = 0.242$ m^2.

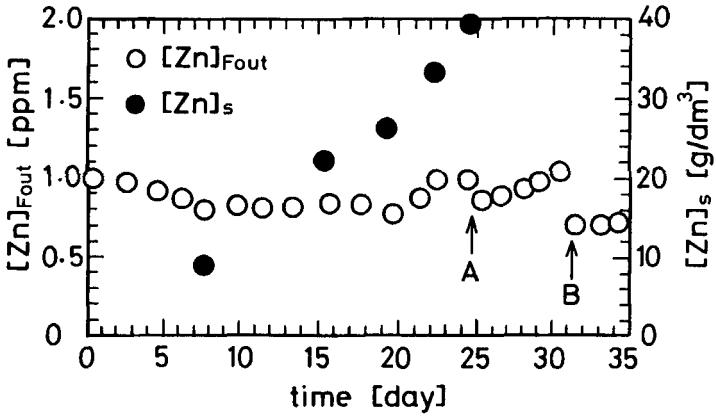

FIG. 17. Life test of Module A and regeneration of degraded membrane. $[(\overline{HL})_2]_0 = 0.698$ mol/dm^3, $[Zn]_{Fin} = 90$ ppm, $pH_{Fin} = 3.00$, $pH_{Fout} = 2.4$, $v_F = 26.5$ cm^3/min. A: Strip solution was replaced by a new solution. B: Regeneration.

determining. As shown in this figure, a significant decrease in the recovery was not recognized for 32 days. As the loss of the organic membrane solution to the aqueous phases by its dissolution has been considered to be the main cause of membrane degradation, regeneration of the membrane was carried out by re-impregnating the module with the organic membrane solution from the strip phase. The membrane was completely regenerated and the permeability of the membrane was restored as shown in Fig. 17. The concentration of zinc in the strip solution, $[Zn]_s$, reached 40 g/dm^3 after 24 days, and the concentration factor $[Zn]_s/[Zn]_{Fout}$ became 40,000.

After the experiment had been continued for 35 days, it was stopped for 40 days with the module filled with the feed and strip solutions. Then the experiment was started again using the same module without washing it. The membrane was found to be degraded because $[Zn]_{Fout}$ was 1.5 ppm, a considerably higher concentration than that shown in Fig. 17. Regeneration was carried out by passing the mixture of the organic membrane phase and the stripping solution through the channel of the strip side. The flow rates of the feed solution and the organic solution were 26.5 and 12 cm^3/min, respectively. $[Zn]_{Fout}$ gradually decreased, and within 2 h it reached 0.9 ppm, which is about the same as the concentration shown in Fig. 17. Thus, the degraded modules can be easily regenerated by flowing the membrane solution alone or by flowing the mixture of the membrane solution and the strip solution in the strip side without interrupting the

permeation of metal ions. This is an advantage of supported liquid membrane operation over ion-exchange operations where adsorption and desorption (regeneration) must be made in a cyclic mode.

To achieve high recovery of permeates and also to treat large amounts of feed solution, the membrane area must be increased. However, too long a channel results in a large pressure drop. To avoid this, use of a multicompartment-type module is desirable where the feed solution is distributed to many channels. One of these is a plate-and-frame-type module where many channels separated by membranes from each other are arranged so that the feed solution and the strip solution flow in neighboring channels. The configuration may be similar to a plate-and-frame-type heat exchanger. Another type of the module is a spiral-type module with many compartments, as schematically shown in Fig. 18. The methods for designing modules and for regenerating degraded modules which have been developed in the present study may also be applicable to these modules.

(4) Comparison of the Experimental Results with Computed Results

To calculate the relation of $[M]_{Fout}/[M]_{Fin}$ vs v_F for each experimental condition, it is necessary to determine or estimate parameters involved in the flux and equilibrium equations.

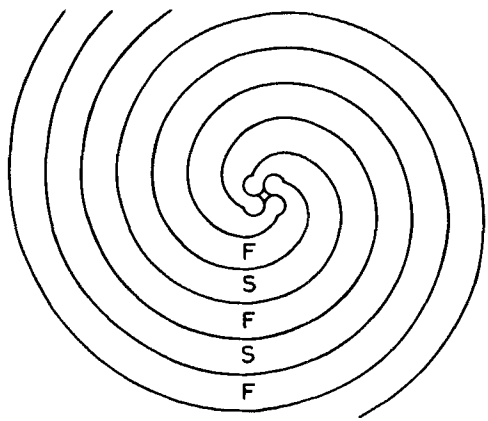

FIG. 18. Spiral-type supported liquid membrane module with many compartments. *F*, feed phase; *S*, strip phase.

The extraction constants for metals-PC-88A systems were experimentally determined, i.e., $K_{exCo} = 4.14 \times 10^{-6}$, $K_{exNi} = 3.13 \times 10^{-7}$ dm^3/mol, $K_{exNa} = 2.0 \times 10^{-5}$ dm^3/mol. Dimerization constant K_2 (diluent: *n*-heptane) was measured by vapor pressure osmometry ($K_2 = 8000$ dm^3/mol) (*10*). It was assumed that k_{FNi} is equal to k_{FCo}, and k_{FNa} is equal to twice the value of k_{FCo}. Mass transfer coefficients in the liquid membrane are dependent on the carrier concentration. The value of k_{mCo} at $[\overline{(HL)_2}]_0 = 0.735$ mol/dm^3 was calculated from J_{Co} obtained in the experiment using the diffusion cell where cobalt was transported from an organic solution loaded with a small amount of cobalt to the strip solution through a microporous membrane. In this case, J_{Co} is expressed by Eq. (32), from which k_{mCo} was calculated.

$$J_{Co} = k_{mCo}[\overline{CoL_2(HL)_2}] \tag{32}$$

k_{mB}, $k_{mB'}$, k_{mNi}, and k_{mNa} were estimated from the value of k_{mCo} using the relation that the diffusivity is proportional to (molar volume)$^{-0.6}$ (*11*). The values of k_{mCoP} and k_{mNiP} were estimated in a similar manner by assuming that the ratios of the molar volume of the aggregate of the complexes to that of $(\overline{HL})_2$ was 3 for cobalt and 5 for nickel (*6*). The parameters when $[\overline{(HL)_2}]$ is 0.735 mol/dm^3 are as follows: $k_{mB} = 1.40 \times 10^{-7}$ m/s, $k_{mB'} = 2.12 \times 10^{-7}$ m/s, $k_{mCo} = k_{mNa} = 9.24 \times 10^{-8}$ m/s, $k_{mNi} = 7.24 \times 10^{-8}$ m/s, $k_{mCoP} = 7.24 \times 10^{-8}$ m/s, and $k_{mNiP} = 5.33 \times 10^{-8}$ m/s. The mass transfer coefficients when $[\overline{(HL)_2}]$ is 0.294 mol/dm^3 were estimated by the Stokes-Einstein equation from the values when $[\overline{(HL)_2}]$ is 0.735 mol/dm^3, i.e., $k_{mB} = 3.43 \times 10^{-7}$ m/s, $k_{mB'} = 5.20 \times 10^{-7}$ m/s, $k_{mCo} = k_{mNa} = 2.27 \times 10^{-7}$ m/s, $k_{mNi} = 1.77 \times 10^{-7}$ m/s, $k_{mCoP} = 1.77 \times 10^{-7}$ m/s, and $k_{mNiP} = 1.31 \times 10^{-7}$ m/s. β_{1Co} and β_{2Co} were determined as 5.5 dm^3/mol and 12.3 dm^6/mol^2, respectively (*6*). For simplicity, it was assumed that β_{1Ni} and β_{2Ni} are equal to β_{1Co} and β_{2Co}, respectively.

K_{exZn} for the zinc-D2EHPA system was determined as 0.063 (mol/dm^3)$^{1/2}$. The value of K_{exNa} reported by Higaki (*12*) was used (4.0×10^{-4} dm^3/mol). The dimerization constant of D2EHPA was measured by VPO ($K_2 = 3 \times 10^4$ dm^3/mol in heptane (*10*)). The value of k_{FH} was taken as approximately five times the value of k_{FZn}. It was confirmed that the computed recovery of zinc was not influenced by the variation of k_{FH} in the range from three times k_{FZn} to ten times k_{FZn}. Mass transfer coefficients in the membranes were estimated by the Stokes-Einstein equation from the values for the metals-PC-88A system, i.e., $k_{mB} = 1.60 \times 10^{-7}$ m/s, $k_{mB'} = 2.42 \times 10^{-7}$ m/s, $k_{mZn} = 1.25 \times 10^{-7}$ m/s, and $k_{mNa} = 1.06 \times 10^{-7}$ m/s.

The solid lines in Figs. 9 and 13-16 are the computed results. The

agreement between the experimental data and the computed results is satisfactory.

CONCLUSION

(1) Experiments on the recovery of cobalt, nickel, and zinc were performed using spiral-type supported liquid membrane modules. It was confirmed that this type of module is very effective in recovering metal ions, and that the degree of recovery reached about 99.99%. Such high recovery is mainly because the flow pattern of the feed phase is very close to plug flow in the module.

(2) Design equations for the spiral-type module were presented. These equations successfully simulate the effect of experimental condition on the recovery of metal ions in their single as well as simultaneous permeation.

(3) The life of the membrane was more than 1 month, and the degraded membranes were easily regenerated by simply passing the organic membrane solutions in the modules.

(4) Spiral-type modules may be used for the recovery of various solutes, including metal ions, as an alternative to such operations as ion exchange and solvent extraction.

SYMBOLS

D	diffusivity of metal in feed phase (m^2/s)
D_M	distribution ratio of metal
d	inner diameter of hollow fiber (m)
I	ionic strength (mol/m^3)
J	flux ($mol/m^2 \cdot s$)
J_{max}	flux obtained when diffusion of carrier in liquid membrane is rate controlling ($mol/m^2 \cdot s$)
K_{ex}	extraction constant
K_2	dimerization constant of carrier (dm^3/mol)
k_F	mass transfer coefficient in boundary layer of feed phase (m/s)
k_{mB}, $k_{mB'}$	mass transfer coefficients of dimer and monomer of carrier in liquid membrane, respectively (m/s)
$k_{m\mathrm{Co}}$, $k_{m\mathrm{Ni}}$	mass transfer coefficients of $\overline{CoL_2(HL)_2}$ and $\overline{NiL_2(HL)_4}$ in liquid membrane, respectively (m/s)

$k_{m\mathrm{CoP}}, k_{m\mathrm{NiP}}$	mass transfer coefficients of aggregates of cobalt-carrier and nickel-carrier complexes in liquid membrane, respectively (m/s)
L	thickness of supported liquid membrane (m)
l	length of hollow fiber (m)
[M]	total metal concentration (mol/m^3)
[M^{n+}]	free metal concentration (mol/m^3)
S	total effective membrane area (m^2)
s	membrane area measured from inlet of feed solution (m^2)
Sh_m	mean Sherwood number
u	average velocity or linear velocity (m/s)
v_F	volumetric feed rate (m^3/s)
x	distance from feed-membrane interface

Subscripts

B	dimer of carrier
B'	monomer of carrier
F	feed solution
Fi	feed-membrane interface
M	metal (Co, Ni, Zn)
m	membrane
S	strip solution
Si	strip-membrane interface
0	initial

Greeks

β_{iM}	stability of constant of reaction $M^{2+} + i\mathrm{OAc}^- \rightleftharpoons M(OAc^-)_i^{2-i}$

Acknowledgments

This work was supported by a Grant-in Aid for Special Research Project on Environmental Science from the Ministry of Education, Culture and Science, Japan in 1985 (No. 58030045) and in 1986 (No. 61030049). We thank Daihachi Chemicals Industry Co., Ltd., Japan, for supplying PC-88A.

REFERENCES

1. R. Marr and A. Kopp, *Chem.-Ing.-Tech., 52,* 390 (1980).
2. W. C. Babcock, R. W. Baker, D. J. Kelly, and E. D. LaChapelle, *Proc. ISEC'80, 2,* 8 (1980).
3. W. C. Babcock, D. J. Kelly, and D. T. Friesen, *Proc. ISEC'83,* p. 373 (1983).
4. P. R. Danesi and P. G. Rickert, *Solvent Extr. Ion Exch., 4,* 149 (1986).
5. D. Pearson, in *Ion Exchange Membranes* (D. S. Flett, ed.), Ellis-Horwood, Chichester, 1983, p. 55.
6. H. Matsuyama, Y. Katayama, A. Kojima, I. Washijima, Y. Miyake, and M. Teramoto, *J. Chem. Eng. Jpn., 20,* 213 (1987).
7. I. Komasawa, T. Otake, and I. Hattori, *Ibid., 16,* 210 (1983).
8. M. Teramoto and H. Tanimoto, *Sep. Sci. Technol., 18,* 871 (1983).
9. H. Hausen, *Verfahrenstechnik Beih. Z. Ver. Deut. Ing., 4,* 91 (1943).
10. Y. Miyake, M. Nishida, M. Nakai, T. Nagata, T. Takeda, and M. Teramoto, *Proc. ISEC'86, DECHEMA,* Vol. 2, Munich, 1986, p. 323.
11. C. R. Wilke and P. Chang, *AIChE J., 1,* 264 (1965).
12. Y. Higaki, MS Thesis, Osaka University, 1980.

Received by editor September 4, 1986